Computer Assisted Methods in Engineering and Science, **19**: 199–212, 2012.

Computational challenges in the simulation of nonlinear electroelasticity

Paul Steinmann, Duc Khoi Vu
Chair of Applied Mechanics, University of Erlangen-Nuremberg
Egerlandstrasse 5, 91058 Erlangen, Germany
e-mail: paul.steinmann@ltm.uni-erlangen.de

Nonlinear electroelasticity is not a new problem, its theory involving nonlinear deformation and nonlinear material behavior has been well established. However, the numerical simulation of nonlinear electroelasticity is until now still far from satisfactory, especially when the interaction between electric fields and matter cannot be considered as confined in the finite space occupied by the matter. It is understood that under the application of an electric field, the deformation of an elastic body is governed not always by what happens inside the material body but in many cases also by the environment surrounding it. This is notably true in the case of electronic electroactive polymers, the materials that emerge today as a leading candidate in developing artificial muscles. In this work, we present a numerical analysis of nonlinear electroelasticity by assuming large deformation, nonlinear polarization and by paying attention to the contribution of the free space surrounding the bodies of interest.

Keywords: nonlinear electricity, nonlinear elasticity, nonlinear coupling, coupled BEM-FEM analysis.

1. Introduction

In nonlinear electroelasticity we study the interaction between polarizable bodies and electric fields. This coupled electro-mechanical phenomenon can be viewed in a simple way as follows: when being immersed in an electric field a polarizable body deforms because of the electric forces acting on electric dipoles that appear together with the application of the electric field or exist already inside the body. The polarization and deformation of the body lead to changes in the electric field and correspondingly to the electric forces, whose changes in turn affect the polarization and deformation. The process continues to take place until a stable state is established. When the body of interest and the electric field can be considered as a close system and the total energy is considered as stored inside the space occupied by the body, a stored energy function can be assumed to be a function of the electric field and the deformation at every point, which helps construct a variational equation for the coupled problem. This variational equation can be discretized by using the finite element method and the system of nonlinear equations obtained from the discretization can be linearized and solved numerically, see for example [7] or [11]. In the case the energy is stored not only inside the body of interest but also in the free space surrounding it (normally air or, as we can in this context consider equivalently, vacuum), the simulation becomes more cumbersome. In this case, as it is well known in the numerical simulation of electric fields, a large finite element mesh can be used to simulate a sufficiently large part of the surrounding space (see for example [3]) or the boundary element method can be employed. When dealing with large deformation, the difficulty in using a large finite element mesh does not lie entirely in the amount of effort that needs to be spent on the computation of the electric field inside this mesh, but also in the effort to remesh the surrounding space after every few iterations. Besides, the construction of such a finite element mesh is not-user friendly since tests must be realized to determine a suitable shape and size for the part of the surrounding space that needs to be taken into account. An alternative method is the

use of a coupled boundary finite element method discussed recently in [8], [9] and [10], in which the finite element method is used to simulate the material body and the boundary element method is used to simulate the finite or infinite free space surrounding the body of interest. In using the boundary element method, the electric field in the free space can be simulated in a very efficient manner. In this work, we use the method proposed in [8] and [9] to investigate the influence of the free space on the electric field and on the deformation field of the body. In what follows, we recall the governing equations of nonlinear electroelasticity, in which the effect of the surrounding space is taken into account with the help of the electric tractions and electric fluxes at the boundary of the material body. These tractions and fluxes will be computed with the help of some boundary integral equations. For the sake of simplicity, we restrict ourselves to the case of static electric loading with no body charge, no current and no magnetic field. No dynamic effect is considered here.

2. Governing equations

Let us consider a body made of elastic material. The undeformed configuration of the body is denoted by $\mathcal{B}_0$. In this configuration the position vector of each point is denoted by $\boldsymbol{X}$. Corresponding to $\mathcal{B}_0$, the deformed configuration of the body under the application of mechanical and electrical forces is denoted by $\mathcal{B}_t$. The position vector of each point in the deformed configuration $\mathcal{B}_t$ is denoted by $\boldsymbol{x}$: $\boldsymbol{x} = \boldsymbol{\varphi}(\boldsymbol{X})$. The deformation of the body at every point inside the body is characterized by the deformation gradient $\boldsymbol{F} = \boldsymbol{F}(\boldsymbol{X}) = \dfrac{\partial \boldsymbol{\varphi}(\boldsymbol{X})}{\partial \boldsymbol{X}}$. In addition, we suppose that the free space $\mathcal{V}_t$ surrounding $\mathcal{B}_t$ has two parts (Fig. 1), a finite part $\mathcal{V}_t^f$ (cavity) and an infinite part $\mathcal{V}_t^i$ such that $\partial\mathcal{B}_t = \partial\mathcal{V}_t^f \cup \partial\mathcal{V}_t^i$. Correspondingly, the two parts of the free space $\mathcal{V}_0$ surrounding $\mathcal{B}_0$ are denoted by $\mathcal{V}_0^f$ and $\mathcal{V}_0^i$ with $\partial\mathcal{B}_0 = \partial\mathcal{V}_0^f \cup \partial\mathcal{V}_0^i$. For later use, we define two coordinate systems with basis vectors $\{\boldsymbol{E}_I, I = 1,2,3\}$ in the undeformed configuration $\mathcal{B}_0$ and $\{\boldsymbol{e}_i, i = 1,2,3\}$ in the deformed configuration $\mathcal{B}_t$. By using these coordinate systems and Einstein's summation convention, the position vectors $\boldsymbol{X}$ and $\boldsymbol{x}$ are expressed as $\boldsymbol{X} = X_I\boldsymbol{E}_I$ and $\boldsymbol{x} = x_i\boldsymbol{e}_i$, while the deformation gradient is presented in the format $\boldsymbol{F} = F_{iJ}(\boldsymbol{X})\boldsymbol{e}_i \otimes \boldsymbol{E}_J$ with the coordinates $F_{iJ}(\boldsymbol{X}) = \dfrac{\partial \varphi_i(\boldsymbol{X})}{\partial X_J}$.

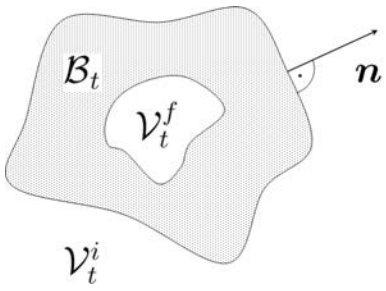

Fig. 1. Infinite ($\mathcal{V}_t^i$) and finite ($\mathcal{V}_t^f$) free space.

Governing equations for the electric field in reference to the deformed configuration. When the body is immersed in an electric field, besides normal mechanical forces, as mentioned above, there are electric forces acting on the electric dipoles that are distributed inside the material body. As the electric body force and the electric traction must be taken into account in the governing equations of the motion problem, the electric field inside and outside the material body must be determined. In reference to the deformed configuration $\mathcal{B}_t$, at every point inside the material body, the electric field is governed by four Maxwell's equations: (1) Gauss' law for electricity that describes how electric charges produce electric fields; (2) Gauss' law for magnetism that describes the experimental absence of magnetic monopoles; (3) Ampere's law that describes how currents

produce magnetic fields; (4) Faraday's law of induction that describes how changing magnetic fields produce electric fields. For the case considered here we assume that there exist no magnetic field, no current and no body charges. By bypassing Gauss's law for magnetism and Ampere's law because of vanishing current and vanishing magnetic field, the spatial electric field vector $\mathbb{e} = \mathbb{e}(\boldsymbol{x}) = \mathrm{e}_i(\boldsymbol{x})\boldsymbol{e}_i$ is determined by Faraday's law of induction

$$\nabla_{\boldsymbol{x}} \times \mathbb{e} = \mathbf{0} \tag{1}$$

and by electric Gauss's law

$$\nabla_{\boldsymbol{x}} \cdot \mathbb{d} = 0, \tag{2}$$

where the spatial electric displacement $\mathbb{d} = \mathbb{d}(\boldsymbol{x}) = \mathrm{d}_i(\boldsymbol{x})\boldsymbol{e}_i$ is computed as a function of the spatial electric field vector $\mathbb{e}$ and the spatial electric polarization $\mathbb{p} = \mathbb{p}(\boldsymbol{x}) = \mathrm{p}_i(\boldsymbol{x})\boldsymbol{e}_i$

$$\mathbb{d} = \epsilon_0 \mathbb{e} + \mathbb{p}, \tag{3}$$

where ϵ_0 is the electric permittivity of vacuum. It should be emphasized that no special assumption about the relationship between the spatial electric polarization $\mathbb{p}$ and the spatial electric field vector $\mathbb{e}$ is made here. For the case of an isotropic material, the spatial electric polarization $\mathbb{p}$ is a nonlinear function of the spatial electric field vector $\mathbb{e}$ and the deformation gradient $\boldsymbol{F}$ or in other words $\mathbb{p} = \mathbb{p}(\mathbb{e}, \boldsymbol{F})$. As consequence, the spatial electric displacement is also a nonlinear function of the electric field and the deformation gradient $\mathbb{d} = \mathbb{d}(\mathbb{e}, \boldsymbol{F})$. For a point lying outside the material body, i.e., in $\mathcal{V}_t$, Faraday's law of induction, electric Gauss's law and the constitutive equation for the spatial electric displacement become

$$\nabla_{\boldsymbol{x}} \times \mathbb{e}^{\epsilon_0} = \mathbf{0}, \qquad \nabla_{\boldsymbol{x}} \cdot \mathbb{d}^{\epsilon_0} = 0 \quad \text{and} \quad \mathbb{d}^{\epsilon_0} = \epsilon_0 \mathbb{e}^{\epsilon_0}, \tag{4}$$

where we use the notation $(\bullet)^{\epsilon_0}$ to denote electric quantities at a point lying in $\mathcal{V}_t$.

For simplicity we assume that inside the material body there is no surface of discontinuity and the jump conditions for mechanical as well as electrical quantities only apply at the boundary of the body. At the boundary of the body $\partial\mathcal{B}_t$, the jump condition for the spatial electric field vector $\mathbb{e}$ and the spatial electric displacement $\mathbb{d}$ are

$$[\![\mathbb{e}]\!] \times \boldsymbol{n} = \mathbf{0} \quad \text{and} \quad [\![\mathbb{d}]\!] \cdot \boldsymbol{n} = -\widehat{\varrho}_t^{\,\mathrm{fre}}, \tag{5}$$

where $\boldsymbol{n} = n_i\boldsymbol{e}_i$ is the unit outward pointing normal to the boundary $\mathcal{B}_t$ and $\widehat{\varrho}_t^{\,\mathrm{fre}}$ is the surface charge density applied on $\partial\mathcal{B}_t$. In the above conditions, the jump $[\![(\bullet)]\!]$ is defined as the change in the value $(\bullet)$ when going from inside the material body to the free space outside $[\![(\bullet)]\!] = (\bullet)_{inside} - (\bullet)_{outside}$. The jump conditions (5) can be also written in the format

$$\mathbb{e} \times \boldsymbol{n} = \mathbb{e}^{\epsilon_0} \times \boldsymbol{n} \quad \text{and} \quad \mathbb{d} \cdot \boldsymbol{n} = q_t - \widehat{\varrho}_t^{\,\mathrm{fre}}, \tag{6}$$

where the electric flux q_t is defined as $q_t = \mathbb{d}^{\epsilon_0} \cdot \boldsymbol{n}$.

In order to solve the problem of finding the electric field, a scalar electric potential $\psi = \psi(\boldsymbol{x})$ (called here spatial electric potential) is defined in such a way that the spatial electric field vector can be computed by the spatial gradient of this potential

$$\mathbb{e} = -\nabla_{\boldsymbol{x}}\psi. \tag{7}$$

By using the spatial electric potential ψ, Faraday's law of induction is satisfied automatically due to the fact that $\nabla_{\boldsymbol{x}} \times \nabla_{\boldsymbol{x}}\psi = \mathbf{0}$. Furthermore, the jump condition $(5)_1$, i.e., $(6)_1$, is also satisfied if ψ is continuous across the boundary of the material body $\mathcal{B}_t$.

Governing equations for the electric field in reference to the undeformed configuration. Corresponding to the above governing equations written in reference to the deformed configuration, in reference to the undeformed configuration, the governing equations for the electric field can be written in terms of the pull-back versions of the spatial electric field vector, spatial electric displacement, spatial electric polarization and spatial electric potential. The pull-back version of the spatial electric field vector $\mathbb{e}$ in $\mathcal{B}_0$ is called the material electric field vector and is denoted by $\mathbb{E}$, which is defined as

$$\mathbb{E} = \boldsymbol{F}^t \cdot \mathbb{e} \tag{8}$$

or in index notation $\mathbb{E} = \mathrm{E}_I \boldsymbol{E}_I$, in which the coordinates E_I are computed by $\mathrm{E}_I = F_{Ij}\mathrm{e}_j$ and e_j are the coordinates of the spatial electric field vector $\mathbb{e}$ as defined above. The pull-back version of the spatial electric field vector $\mathbb{d}$ in $\mathcal{B}_0$ is called the material electric displacement vector and is denoted by $\mathbb{D}$. This vector is defined by

$$\mathbb{D} = J\boldsymbol{F}^{-1} \cdot \mathbb{d} \tag{9}$$

or in index notation $\mathbb{D} = \mathrm{D}_I \boldsymbol{E}_I$, where $\mathrm{D}_I = JF^{-1}_{Ij}\mathrm{d}_j$ and d_j are the coordinates of the spatial electric displacement vector $\mathbb{d}$. By using the above definitions of the material electric field vector $\mathbb{E}$ and the material electric displacement vector $\mathbb{D}$, Faraday's law of induction is now written in reference to the undeformed configuration $\mathcal{B}_0$ as

$$\nabla_{\boldsymbol{X}} \times \mathbb{E} = \boldsymbol{0} \tag{10}$$

and electric Gauss's law becomes

$$\nabla_{\boldsymbol{X}} \cdot \mathbb{D} = 0. \tag{11}$$

Also by using the above definitions of the material electric field vector $\mathbb{E}$ and the material electric displacement vector $\mathbb{D}$, the relationship (3) can be rewritten in the format

$$\mathbb{D} = \epsilon_0 J\boldsymbol{C}^{-1} \cdot \mathbb{E} + J\boldsymbol{F}^{-1} \cdot \mathbb{p}, \tag{12}$$

which motivates the definition of the material polarization $\mathbb{P}$ as

$$\mathbb{P} = J\boldsymbol{F}^{-1} \cdot \mathbb{p} \tag{13}$$

or in index notation $\mathbb{P} = \mathrm{P}_I \boldsymbol{E}_I$, where $\mathrm{P}_I = JF^{-1}_{Ij}\mathrm{p}_j$. It should be noted that this definition of the material polarization is not unique and other versions are possible.

In reference to the undeformed configuration $\mathcal{B}_0$, the jump conditions for the material electric field vector $\mathbb{E}$ and the material electric displacement $\mathbb{D}$ at the boundary $\partial\mathcal{B}_0$ are written in the format

$$[\![\mathbb{E}]\!] \times \boldsymbol{N} = \boldsymbol{0} \quad \text{and} \quad [\![\mathbb{D}]\!] \cdot \boldsymbol{N} = -\widehat{\varrho}_0^{\,\mathrm{fre}} \tag{14}$$

or in the format

$$\mathbb{E} \times \boldsymbol{N} = \mathbb{E}^{\epsilon_0} \times \boldsymbol{N} \quad \text{and} \quad \mathbb{D} \cdot \boldsymbol{N} = q_0 - \widehat{\varrho}_0^{\,\mathrm{fre}}, \tag{15}$$

where $q_0 = \mathbb{D}^{\epsilon_0} \cdot \boldsymbol{N}$, $\boldsymbol{N} = N_I \boldsymbol{E}_I$ is the unit outward pointing normal to the boundary $\mathcal{B}_0$ and $\widehat{\varrho}_0^{\,\mathrm{fre}}$ is the surface charge density applied on $\partial\mathcal{B}_0$.

Corresponding to the spatial electric potential $\psi = \psi(\boldsymbol{x})$, in reference to the undeformed configuration $\mathcal{B}_0$ we define the material electric potential $\Psi = \Psi(\boldsymbol{X})$ such that $\Psi(\boldsymbol{X}) = \psi(\boldsymbol{x}) \circ \boldsymbol{\varphi}(\boldsymbol{X})$. With this definition of the material electric potential, the material electric field vector is computed as

$$\mathbb{E} = -\nabla_{\boldsymbol{X}} \Psi. \tag{16}$$

By using the material electric potential Ψ, Faraday's law of induction (10) is satisfied automatically due to the fact that $\nabla_{\boldsymbol{X}} \times \nabla_{\boldsymbol{X}} \Psi = \boldsymbol{0}$ and the jump condition $(14)_1$, or equivalently $(15)_1$, is also satisfied if Ψ is continuous across the boundary of the material body $\mathcal{B}_0$. Furthermore, the use of the relationship $\Psi(\boldsymbol{X}) = \psi(\boldsymbol{x}) \circ \boldsymbol{\varphi}(\boldsymbol{X})$ is compatible with the pull-back formulation (8) since $\nabla_{\boldsymbol{X}} \Psi = \nabla_{\boldsymbol{x}} \psi \cdot \boldsymbol{F}$. For further details on the governing equations of electric fields, see for example [5].

Governing equations for the mechanical field in reference to the deformed configuration. In reference to the spatial configuration $\mathcal{B}_t$ if we denote the electric body force that an electric field exerts on material by $\boldsymbol{b}_t^{\text{ele}} = \boldsymbol{b}_t^{\text{ele}}(\boldsymbol{x}) = b_{ti}^{\text{elec}}(\boldsymbol{x}) \boldsymbol{e}_i$, the balance equation of linear momentum is written as

$$\nabla_{\boldsymbol{x}} \cdot \boldsymbol{\sigma}^t + \boldsymbol{b}_t^{\text{mec}} + \boldsymbol{b}_t^{\text{ele}} = \boldsymbol{0}, \tag{17}$$

where $\boldsymbol{\sigma} = \boldsymbol{\sigma}(\boldsymbol{x}) = \sigma_{ij}(\boldsymbol{x}) \boldsymbol{e}_i \otimes \boldsymbol{e}_j$ is the Cauchy stress tensor, $\boldsymbol{\sigma}^t$ is the transpose of $\boldsymbol{\sigma}$ and $\boldsymbol{b}_t^{\text{mec}} = \boldsymbol{b}_t^{\text{mec}}(\boldsymbol{x}) = b_{ti}^{\text{mec}}(\boldsymbol{x}) \boldsymbol{e}_i$ denotes the mechanical body force. The electric body force $\boldsymbol{b}_t^{\text{ele}}$ can be computed as a function of the electric field vector $\mathbb{e}$ and the electric polarization vector $\mathbb{p}$ in the format

$$\boldsymbol{b}_t^{\text{ele}} = [\nabla_{\boldsymbol{x}} \mathbb{e}] \cdot \mathbb{p}. \tag{18}$$

Note that the balance equation of linear momentum (17) is the same as that of a normal nonlinear elastic system, except the fact that the Cauchy stress tensor here is not symmetric. This can be seen by considering the balance equation of angular momentum and by noting that the electric body force $\boldsymbol{b}_t^{\text{ele}}$ can be written as the divergence of stress like tensor $\boldsymbol{\sigma}^{\text{ele}}$ in the format

$$\boldsymbol{b}_t^{\text{ele}} = \nabla_{\boldsymbol{x}} \cdot \boldsymbol{\sigma}^{\text{ele},t}, \tag{19}$$

in which $\boldsymbol{\sigma}^{\text{ele}}$ is called here the electric stress tensor and is defined as

$$\boldsymbol{\sigma}^{\text{ele}} = \mathbb{d} \otimes \mathbb{e} - \frac{1}{2} \epsilon_0 [\mathbb{e} \cdot \mathbb{e}] \boldsymbol{i}, \tag{20}$$

where $\boldsymbol{i}$ is the second unit tensor $\boldsymbol{i} = \delta_{ij} \boldsymbol{e}_i \otimes \boldsymbol{e}_j$. Note that the above definition of the electric stress tensor $\boldsymbol{\sigma}^{\text{ele}}$ is chosen for the sake of simplicity. This is due to the fact that the electric stress tensor $\boldsymbol{\sigma}^{\text{ele}}$ satisfying the Eq. (19) is only defined up to an additive constant. For the case of linear polarization, the electric displacement vector $\mathbb{d}$ and the electric field vector are parallel as the consequence of the relationship $\mathbb{d} = \epsilon_m \mathbb{e}$ (where ϵ_m is the electric permittivity of the material body), the electric stress tensor $\boldsymbol{\sigma}^{\text{ele}}$ as defined by (20) is therefore symmetric. In this case the use of the balance equation of angular momentum leads to the requirement that the Cauchy stress tensor is symmetric. In the more general case, in which the electric displacement vector is a nonlinear function of the electric field, the electric field vector $\mathbb{e}$ and the electric displacement vector $\mathbb{d}$ are not parallel. The use of the balance equation of angular momentum in this case requires that not the Cauchy stress tensor $\boldsymbol{\sigma}$, but the combination of $\boldsymbol{\sigma}$ and $\boldsymbol{\sigma}^{\text{ele}}$ must be symmetric. This requirement gives us the reason to define a total stress tensor $\boldsymbol{\sigma}^{\text{tot}}$ in the format (see [4] or [6])

$$\boldsymbol{\sigma}^{\text{tot}} = \boldsymbol{\sigma} + \boldsymbol{\sigma}^{\text{ele}}. \tag{21}$$

Note that in the free space $\mathcal{V}_t$ surrounding the body of interest, the Cauchy stress tensor vanishes and the total stress tensor $\boldsymbol{\sigma}^{\text{tot}}$ reduces to the well-known Maxwell stress tensor

$$\boldsymbol{\sigma}^{\max} = \epsilon_0 \left[\mathbb{e}^{\epsilon_0} \otimes \mathbb{e}^{\epsilon_0} - \frac{1}{2} \left[\mathbb{e}^{\epsilon_0} \cdot \mathbb{e}^{\epsilon_0} \right] \boldsymbol{i} \right]. \tag{22}$$

By using the total stress tensor $\boldsymbol{\sigma}^{\text{tot}}$, the balance equation of linear momentum now has the same format as what we have for the case of a normal nonlinear system

$$\nabla_{\boldsymbol{x}} \cdot \boldsymbol{\sigma}^{\text{tot},t} + \boldsymbol{b}_t^{\text{mec}} = \boldsymbol{0}, \tag{23}$$

where $\boldsymbol{\sigma}^{\mathrm{tot},t}$ is the transpose of $\boldsymbol{\sigma}^{\mathrm{tot}}$. At the boundary $\partial\mathcal{B}_t$, the total stress tensor $\boldsymbol{\sigma}^{\mathrm{tot}}$ must satisfy the jump condition

$$[\![\boldsymbol{\sigma}^{\mathrm{tot}}]\!] \cdot \boldsymbol{n} = \boldsymbol{t}_t^{\mathrm{mec}}, \tag{24}$$

where $\boldsymbol{t}_t^{\mathrm{mec}}$ is the mechanical traction acting on $\partial\mathcal{B}_t$. The above jump condition takes into account both the contribution of the Cauchy stress tensor $\boldsymbol{\sigma}$ and the contribution of the electric stress tensor $\boldsymbol{\sigma}^{\mathrm{ele}}$ and is therefore preferred over the jump condition for the Cauchy stress tensor. By noting that in the free space outside the body of interest $\boldsymbol{\sigma}^{\mathrm{tot}} = \boldsymbol{\sigma}^{\max}$, the jump condition (24) can be written as

$$\boldsymbol{\sigma}^{\mathrm{tot}} \cdot \boldsymbol{n} = \boldsymbol{t}_t^{\mathrm{mec}} + \boldsymbol{t}_t^{\max}, \tag{25}$$

where $\boldsymbol{t}_t^{\max} = \boldsymbol{\sigma}^{\max} \cdot \boldsymbol{n}$ is the electric traction or Maxwell's traction. The importance of the electric traction depends on the material properties of the body. In the case this traction must be taken into account, the boundary condition for the total stress tensor makes the problem more difficult to solve because the evaluation of $\boldsymbol{t}_t^{\max}$ requires the knowledge about the electric field in the free space $\mathcal{V}_t$.

Governing equations for the mechanical field in reference to the undeformed configuration. In reference to the undeformed configuration $\mathcal{B}_0$, the balance equation of linear momentum is written in terms of the Piola stress tensor as

$$\nabla_{\boldsymbol{X}} \cdot \boldsymbol{P} + \boldsymbol{b}_0^{\mathrm{mec}} + \boldsymbol{b}_0^{\mathrm{ele}} = \boldsymbol{0}, \tag{26}$$

where the body forces $\boldsymbol{b}_0^{\mathrm{mec}}$ and $\boldsymbol{b}_0^{\mathrm{ele}}$ are defined as $\boldsymbol{b}_0^{\mathrm{mec}} = J\boldsymbol{b}_t^{\mathrm{mec}}$ and $\boldsymbol{b}_0^{\mathrm{ele}} = J\boldsymbol{b}_t^{\mathrm{elec}}$ where J is the determinant of the deformation gradient $J = \det \boldsymbol{F}$. The Piola stress tensor is considered as the pull-back version of the Cauchy stress tensor in the undeformed configuration $\mathcal{B}_0$

$$\boldsymbol{P} = J\boldsymbol{\sigma} \cdot \boldsymbol{F}^{-t} \tag{27}$$

or $\boldsymbol{P} = P_{iJ}\boldsymbol{e}_i \otimes \boldsymbol{E}_J$ with the coordinates $P_{iJ} = J\sigma_{ik}F_{kJ}^{-t}$. The electric body force can be written in reference to the undeformed configuration $\mathcal{B}_0$ as

$$\boldsymbol{b}_0^{\mathrm{ele}} = \nabla_{\boldsymbol{X}} \left[\boldsymbol{F}^{-t} \cdot \mathbb{E}\right] \cdot \mathbb{P} \tag{28}$$

or as the divergence of a stress like tensor $\boldsymbol{b}_0^{\mathrm{ele}} = \nabla_{\boldsymbol{X}} \cdot \boldsymbol{P}^{\mathrm{ele}}$ with

$$\boldsymbol{P}^{\mathrm{ele}} = \boldsymbol{F}^{-t} \cdot \mathbb{E} \otimes \mathbb{D} - \frac{1}{2}\epsilon_0 J \left[\mathbb{E} \cdot \boldsymbol{C}^{-1} \cdot \mathbb{E}\right] \boldsymbol{F}^{-t}, \tag{29}$$

where $\boldsymbol{C} = \boldsymbol{F}^t \cdot \boldsymbol{F}$ is the right Cauchy-Green strain tensor. Corresponding to the definition of the total stress tensor $\boldsymbol{\sigma}^{\mathrm{tot}}$, in reference to the undeformed configuration, by using the definition of the total stress tensor $\boldsymbol{P}^{\mathrm{tot}}$

$$\boldsymbol{P}^{\mathrm{tot}} = \boldsymbol{P} + \boldsymbol{P}^{\mathrm{ele}} \tag{30}$$

the balance equation of linear momentum is now written as

$$\nabla_{\boldsymbol{X}} \cdot \boldsymbol{P}^{\mathrm{tot}} + \boldsymbol{b}_0^{\mathrm{mec}} = \boldsymbol{0} \tag{31}$$

and the jump condition that this total stress tensor must satisfy at the boundary $\partial\mathcal{B}_0$ reads

$$[\![\boldsymbol{P}^{\mathrm{tot}}]\!] \cdot \boldsymbol{N} = \boldsymbol{t}_0^{\mathrm{mec}} \tag{32}$$

or equivalently

$$\boldsymbol{P}^{\mathrm{tot}} \cdot \boldsymbol{N} = \boldsymbol{t}_0^{\mathrm{mec}} + \boldsymbol{t}_0^{\max}, \tag{33}$$

where $\boldsymbol{t}_0^{\max} = \boldsymbol{P}^{\max} \cdot \boldsymbol{N}$ is the electric traction acting on $\partial\mathcal{B}_0$. From the definitions (27) and (29), it is easy to see that the total stress tensor $\boldsymbol{P}^{\mathrm{tot}}$ can also be considered as the pull-back version of its counterpart $\boldsymbol{\sigma}^{\mathrm{tot}}$ in the undeformed configuration $\mathcal{B}_0$

$$\boldsymbol{P}^{\mathrm{tot}} = J\boldsymbol{\sigma}^{\mathrm{tot}} \cdot \boldsymbol{F}^{-t}. \tag{34}$$

3. Variational formulations and boundary integral equations

Variational formulation in reference to the deformed configuration. In reference to the deformed configuration $\mathcal{B}_t$, the governing equations of the problem, i.e., the balance equations and boundary conditions presented above, can be derived by considering the following variational equation written in terms of the deformation map $\boldsymbol{\varphi} = \boldsymbol{\varphi}(\boldsymbol{X})$ and the spatial electric potential $\psi = \psi(\boldsymbol{x})$

$$\delta \int\limits_{\mathcal{B}_t} \widehat{W}_{t\boldsymbol{F}}\, \mathrm{d}v - \int\limits_{\mathcal{B}_t} \boldsymbol{b}_t^{\mathrm{mec}} \cdot \delta\boldsymbol{\varphi}\, \mathrm{d}v - \int\limits_{\partial\mathcal{B}_t} [\boldsymbol{t}_t^{\mathrm{mec}} + \boldsymbol{t}_t^{\mathrm{max}}] \cdot \delta\boldsymbol{\varphi}\, \mathrm{d}s + \int\limits_{\partial\mathcal{B}_t} \delta\psi[-q_t + \widehat{\varrho}_t^{\,\mathrm{fre}}]\, \mathrm{d}s = 0. \tag{35}$$

In the above equation, $\widehat{W}_{t\boldsymbol{F}} = \widehat{W}_{t\boldsymbol{F}}(\boldsymbol{F}, \mathbb{E})$ is the stored energy density function per unit volume of the deformed configuration. The first term of this equation is the first variation with respect to a change in the motion map $\delta\boldsymbol{\varphi}$ and a change in the spatial electric potential $\delta\psi$ at a fixed material placement, i.e., at $\delta\boldsymbol{X} = \boldsymbol{0}$. By requiring the above equation to hold for an arbitrary change $\delta\boldsymbol{\varphi} \neq \boldsymbol{0}$ and by localizing the result we get the balance equation

$$\nabla_{\boldsymbol{x}} \cdot \left[\widehat{W}_{t\boldsymbol{F}} \boldsymbol{i} + \frac{\partial \widehat{W}_{t\boldsymbol{F}}}{\partial \boldsymbol{F}} \cdot \boldsymbol{F}^t \right] + \boldsymbol{b}_t^{\mathrm{mec}} = \boldsymbol{0} \quad \text{in} \quad \mathcal{B}_t \tag{36}$$

and the boundary condition

$$\left[\widehat{W}_{t\boldsymbol{F}} \boldsymbol{i} + \frac{\partial \widehat{W}_{t\boldsymbol{F}}}{\partial \boldsymbol{F}} \cdot \boldsymbol{F}^t \right] \cdot \boldsymbol{n} = \boldsymbol{t}_t^{\mathrm{mec}} + \boldsymbol{t}_t^{\mathrm{max}} \quad \text{on} \quad \partial\mathcal{B}_t. \tag{37}$$

The comparison of the above balance equation and boundary condition with the balance equation of linear momentum (23) and the boundary condition (25) brings us to define the total stress tensor $\boldsymbol{\sigma}^{\mathrm{tot}}$ as

$$\boldsymbol{\sigma}^{\mathrm{tot}} := \left[\widehat{W}_{t\boldsymbol{F}} \boldsymbol{i} + \frac{\partial \widehat{W}_{t\boldsymbol{F}}}{\partial \boldsymbol{F}} \cdot \boldsymbol{F}^t \right]^t. \tag{38}$$

By requiring Eq. (35) to hold for an arbitrary change $\delta\psi \neq 0$ and by localizing the result we get the balance equation

$$\nabla_{\boldsymbol{x}} \cdot \left[-\frac{\partial \widehat{W}_{t\boldsymbol{F}}}{\partial \mathbb{e}} \right] = 0 \quad \text{in} \quad \mathcal{B}_t \tag{39}$$

and the boundary condition

$$-\frac{\partial \widehat{W}_{t\boldsymbol{F}}}{\partial \mathbb{e}} \cdot \boldsymbol{n} = q_t - \widehat{\varrho}_t^{\,\mathrm{fre}} \quad \text{on} \quad \partial\mathcal{B}_t, \tag{40}$$

which, by comparing with the balance equation (2) and boundary condition (6.2), prompts us to define the spatial electric displacement as

$$\mathbb{d} := -\frac{\partial \widehat{W}_{t\boldsymbol{F}}}{\partial \mathbb{e}}. \tag{41}$$

Variational formulation in reference to the undeformed configuration. In reference to the undeformed configuration $\mathcal{B}_0$, we consider the following variational equation written in terms of the deformation map $\boldsymbol{\varphi} = \boldsymbol{\varphi}(\boldsymbol{X})$ and the material electric potential $\Psi = \Psi(\boldsymbol{X})$

$$\delta \int\limits_{\mathcal{B}_0} \widehat{W}_0 \boldsymbol{F}\, \mathrm{d}V - \int\limits_{\mathcal{B}_0} \boldsymbol{b}_0^{\mathrm{mec}} \cdot \delta\boldsymbol{\varphi}\, \mathrm{d}V - \int\limits_{\partial\mathcal{B}_0} [\boldsymbol{t}_0^{\mathrm{mec}} + \boldsymbol{t}_0^{\mathrm{max}}] \cdot \delta\boldsymbol{\varphi}\, \mathrm{d}S + \int\limits_{\partial\mathcal{B}_0} \delta\Psi[-q_0 + \widehat{\varrho}_0^{\,\mathrm{fre}}]\, \mathrm{d}S = 0, \tag{42}$$

where $\widehat{W}_{0\boldsymbol{F}} = \widehat{W}_{0\boldsymbol{F}}(\boldsymbol{F}, \mathbb{E})$ is the stored energy density function per unit volume of the undeformed configuration such that $\widehat{W}_{0\boldsymbol{F}} = J\widehat{W}_{t\boldsymbol{F}}$. The first term of the above equation is the first variation with respect to a change in the motion map $\delta\boldsymbol{\varphi}$ and a change in the material electric potential $\delta\Psi$ at a fixed material placement $\delta\boldsymbol{X} = \boldsymbol{0}$. By requiring the above equation to hold for an arbitrary change $\delta\boldsymbol{\varphi} \neq \boldsymbol{0}$ and by localizing the result we get the balance equation

$$\nabla_{\boldsymbol{X}} \cdot \frac{\partial \widehat{W}_{0\boldsymbol{F}}}{\partial \boldsymbol{F}} + \boldsymbol{b}_0^{\mathrm{mec}} = \boldsymbol{0} \quad \text{in} \quad \mathcal{B}_0 \tag{43}$$

and the boundary condition

$$\frac{\partial \widehat{W}_{0\boldsymbol{F}}}{\partial \boldsymbol{F}} \cdot \boldsymbol{N} = \boldsymbol{t}_0^{\mathrm{mec}} + \boldsymbol{t}_0^{\max} \quad \text{on} \quad \partial\mathcal{B}_0. \tag{44}$$

The comparison of the above balance equation and boundary condition with the balance equation of linear momentum (31) and the boundary condition (33) brings us to define the total stress tensor $\boldsymbol{P}^{\mathrm{tot}}$ as

$$\boldsymbol{P}^{\mathrm{tot}} := \frac{\partial \widehat{W}_{0\boldsymbol{F}}}{\partial \boldsymbol{F}}. \tag{45}$$

Note that the definitions of the spatial and material stresses $\boldsymbol{\sigma}^{\mathrm{tot}}$ and $\boldsymbol{P}^{\mathrm{tot}}$ in terms of the stored energy density functions $\widehat{W}_{t\boldsymbol{F}}$ and $\widehat{W}_{0\boldsymbol{F}}$ are compatible with the pull-back formulation (34).

By requiring Eq. (35) to hold for an arbitrary change $\delta\Psi \neq 0$ and by localizing the result we get the balance equation

$$\nabla_{\boldsymbol{X}} \cdot \left[-\frac{\partial \widehat{W}_{0\boldsymbol{F}}}{\partial \mathbb{E}} \right] = 0 \quad \text{in} \quad \mathcal{B}_0 \tag{46}$$

and the boundary condition

$$-\frac{\partial \widehat{W}_{0\boldsymbol{F}}}{\partial \mathbb{E}} \cdot \boldsymbol{N} = q_0 - \widehat{\varrho}_0^{\,\mathrm{fre}} \quad \text{on} \quad \partial\mathcal{B}_0, \tag{47}$$

which, by comparing with the balance equation (11) and boundary condition $(15)_2$, motivates us to define the material electric displacement as

$$\mathbb{D} := -\frac{\partial \widehat{W}_{0\boldsymbol{F}}}{\partial \mathbb{E}}. \tag{48}$$

Again we note that, as in the case of stresses, the definitions of the spatial and material electric displacements $\mathbb{d}$ and $\mathbb{D}$ in terms of the stored energy density functions $\widehat{W}_{t\boldsymbol{F}}$ and $\widehat{W}_{0\boldsymbol{F}}$ are fully compatible with the pull-back formulation (13).

By using the two variational formulations (34) and (42) the problem of finding the motion map $\boldsymbol{\varphi}$ and the electric potential ψ (or Ψ) can be solved with the help of the finite element method provided that the electric surface tractions $\boldsymbol{t}_t^{\max}$, $\boldsymbol{t}_0^{\max}$ and the electric surface fluxes q_t, q_0 are negligible or taken into account by, as mentioned above, using a sufficiently large finite element mesh around the body of interest or by using the boundary element method. In using the boundary element method, the electric field in the free space surrounding the material body is modeled by the following boundary integral equations

$$\psi(\boldsymbol{\xi}) - \psi_\infty - \int_{\partial\mathcal{B}_t} [\psi(\boldsymbol{x}) - \psi(\boldsymbol{\xi})] \frac{\partial G(\boldsymbol{\xi}, \boldsymbol{x})}{\partial n} ds - \int_{\partial\mathcal{B}_t} \frac{q_t}{\epsilon_0} G(\boldsymbol{\xi}, \boldsymbol{x}) ds = 0 \tag{49}$$

and

$$\int_{\partial\mathcal{B}_t} q_t ds = 0, \tag{50}$$

where ψ_∞ is the electric potential at infinity, $\boldsymbol{x}$ is called the field point, $\boldsymbol{\xi}$ is the source point, $\dfrac{\partial[\bullet]}{\partial n}$ is the directional derivative along the unit normal vector $\boldsymbol{n}$ of the boundary and $G(\boldsymbol{\xi}, \boldsymbol{x})$ is the so-called fundamental solution. Note that the boundary integral Eq. (49) is written for the case in which the free space outside the material body is infinite. In the case of finite free space, the above equation should be modified accordingly, namely the first two terms of this equation should be removed. Note also that Eq. (50) represents our assumption that the total free charge of the system is zero.

4. Numerical study

For the numerical simulation, the formulations presented in the previous sections are discretized using the finite element method and the boundary element method. Namely the finite element method is used to discretize the variational equation (35) (or (42)) and the boundary element method is used to discretize the boundary integral equations (49) and (50). The resulting system of equations obtained from the discretization is then a nonlinear system of equations with unknowns being the nodal values of the nonlinear motion map $\boldsymbol{\varphi}$, the electric potential ψ (or Ψ) and the electric flux q_t (or q_0). This nonlinear system can then be solved, for example, using the Newton-Raphson method. For more details on the discretization using the finite element method see for example [2] and for more details on the discretization using the boundary element method see [1] or [12]. By using this procedure, in this section, we study the influence of the free space on the electric field as well as the deformation field inside a C-shaped plate presented in Fig. 2. The width of the plate is $w = 60$ μm, the height is $h = 45$ μm and the thickness is $t = 15$ μm. The electric loading is applied on the structure by means of prescribed electric potentials, in the first case (ψ_{lower} and ψ_{upper}) given on the lower and upper edges of the plate and in the second case (ψ_{in} and ψ_{ex}) given on the internal and external edges of the plate. For the purpose of demonstration, the material properties are given through the stored energy density function $\widehat{W}_{0\boldsymbol{F}}$ defined here in the following format:

$$\widehat{W}_{0\boldsymbol{F}} = \frac{\mu}{2}\left[\boldsymbol{C} : \boldsymbol{I} - 3\right] - \mu \ln J + \frac{\lambda}{2}\left[\ln J\right]^2 + \alpha \boldsymbol{I} : [\mathbb{E} \otimes \mathbb{E}] + \beta \boldsymbol{C} : [\mathbb{E} \otimes \mathbb{E}] - \frac{1}{2}\epsilon_m J \boldsymbol{C}^{-1} : [\mathbb{E} \otimes \mathbb{E}], \tag{51}$$

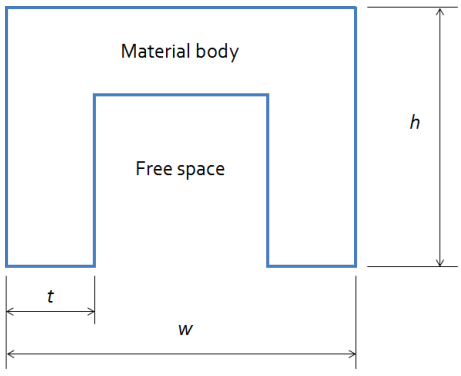

Fig. 2. Material body and free space.

where $\mu = 0.05$ MPa, $\lambda = 0.06$ MPa, $\alpha = 0.2\epsilon_0$, $\beta = 2\epsilon_0$, and $\epsilon_0 = 8.854 \times 10^{-12}$ F/m. Note that the first part of this stored energy density function is the classical neo-Hookean energy density function, the second part with two coefficients α and β is the electro-mechanical coupling and the last part is added to reflect the linear part of the electric polarization, which means that in the case the nonlinear coupling part is neglected by setting both $\alpha = 0$ and $\beta = 0$, the spatial electric polarization is a linear function of the spatial electric field vector or in other words the spatial electric displacement vector is a linear function of the spatial electric field vector $\mathbb{d} = \epsilon_m \mathbb{e}$. By using this stored energy density function and in the absence of the electric field, the material behaves as a neo-Hookean material in nonlinear elasticity. Under the application of an external electric field, the electro-mechanical coupling is the function of the three parameters α, β and ϵ_m. In what follows we will investigate the influence of the free space surrounding the body by assuming that the two parameters α and β are constant as given above and by varying the electric permittivity ϵ_m of the material body.

In this investigation, the simulation of the plate is carried out by using two approaches. In the first approach, only the plate is simulated using finite elements, i.e. only the variational formulation for the material body (35) or (42) is used and the contribution of the free space surrounding the material body is ignored by setting the electric surface tractions $\boldsymbol{t}_t^{\max}$, $\boldsymbol{t}_0^{\max}$ and the electric surface charges q_t, q_0 to zero. The first approach is called FEM approach. In the second approach both the plate and the free space are simulated. The plate is taken into account by the discretized versions of the variational formulations using finite elements. The free space is taken into account by the discretized versions of the boundary integral Eqs. (49) and (50) using boundary elements. The second approach is called here coupled BEM-FEM approach. The mesh used in the FEM simulation is presented in Fig. 3 with 200 four-node quadrangular elements. In the coupled BEM-FEM approach, the same FEM mesh is used for the plate but on the boundary of the FEM mesh, 90 linear two-node boundary elements are used to simulate the contribution of the space surrounding the plate. Note that these boundary elements are constructed automatically using the nodal coordinates of existing finite elements.

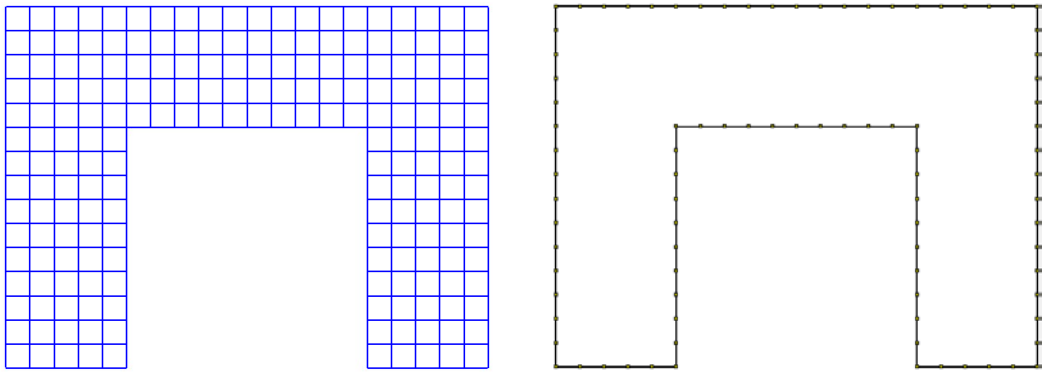

Fig. 3. Finite element mesh (left) and boundary element mesh (right).

In order to study the influence of the free space on the electric field inside the structure, we will consider the first loading case. Here we will first assume that no deformation takes place inside the structure. For this purpose, the displacement of all nodes is set to zero. The simulation results are presented in Figs. 4–7 for different values of the electric permittivity ranging from $\epsilon_m = 5\epsilon_0$ to $\epsilon_m = 1000\epsilon_0$. An electric potential difference of 200 V is placed between the upper and lower edges of the plate by setting $\psi_{upper} = 100\ V$ and $\psi_{lower} = -100\ V$. The simulation results show a clear difference between the results obtained by using the coupled BEM-FEM approach and the FEM approach: the smaller the electric permittivity the larger the difference. For very small electric permittivity (for example in the case of electronic electroactive polymers), the large difference between the two approaches leads to the conclusion that in order to simulate accurately the electric

field inside the material body the influence of the free space must be taken into account. However, for considerably higher electric permittivity (for example in the case of piezoelectric materials), the free space can be conveniently ignored due to its small contribution.

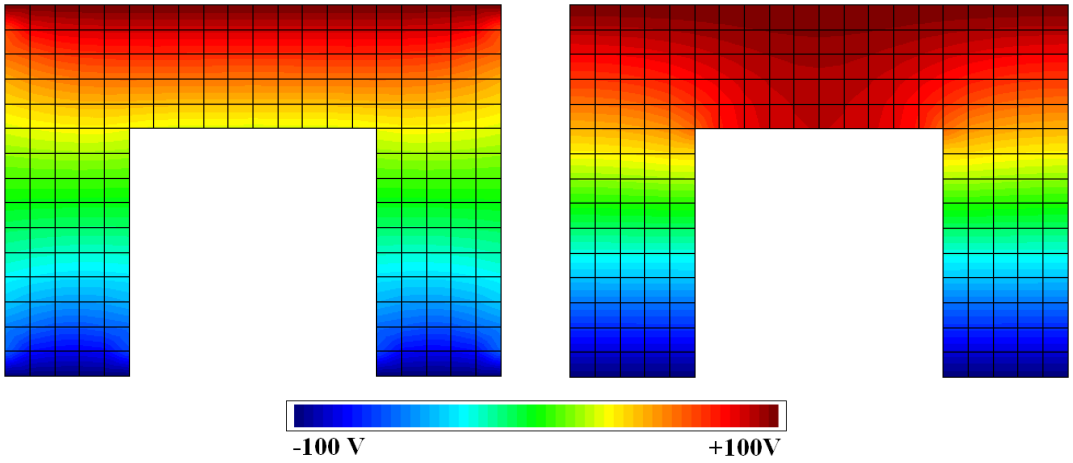

Fig. 4. Electric potential using coupled BEM-FEM (left) and FEM (right): $\epsilon_m = 5.0\epsilon_0$.

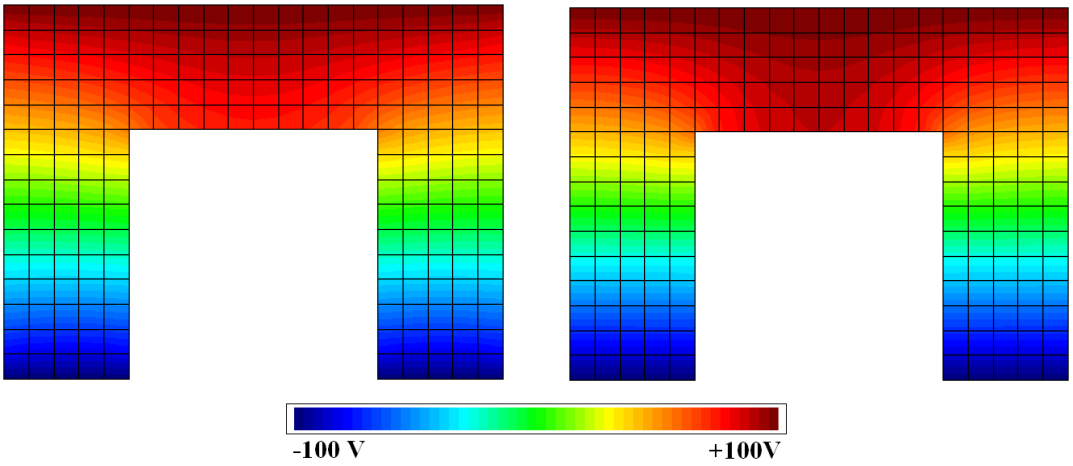

Fig. 5. Electric potential using coupled BEM-FEM (left) and FEM (right): $\epsilon_m = 10.0\epsilon_0$.

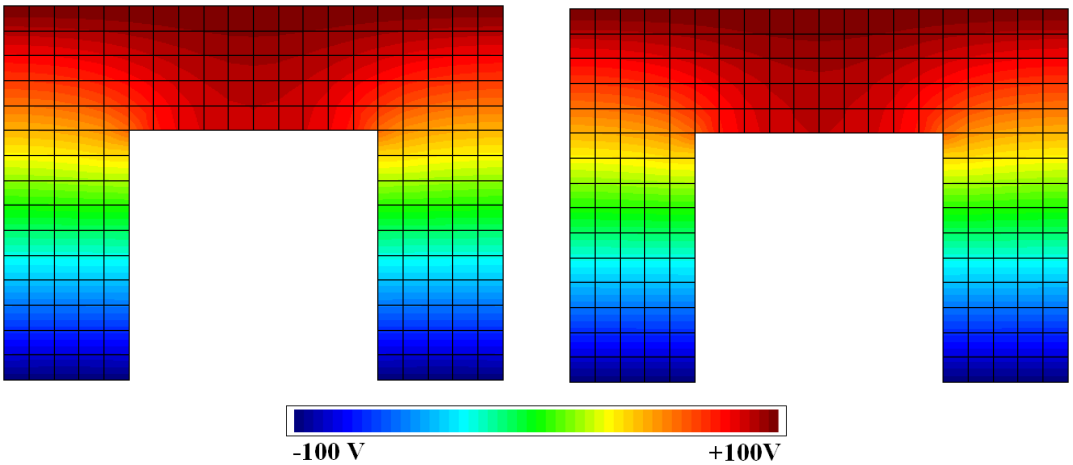

Fig. 6. Electric potential using coupled BEM-FEM (left) and FEM (right): $\epsilon_m = 100.0\epsilon_0$.

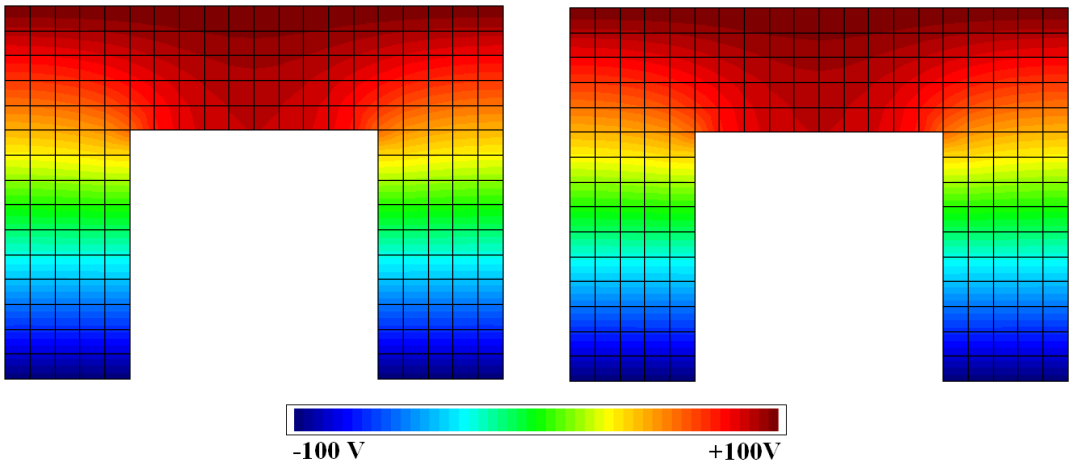

Fig. 7. Electric potential using coupled BEM-FEM (left) and FEM (right): $\epsilon_m = 1000.0\epsilon_0$.

For the analysis of the influence of the free space on both the electric field and the deformation field inside the structure, we again consider the first loading case. Here we assume that the nodal displacement of all nodes lying on the symmetric plane of the plate is set to zero in the horizontal direction. Furthermore, the nodal displacement of all nodes lying on the lower edges of the plate is set to zero in the vertical direction. The numerical results obtained using the two approaches are presented in Figs. 8–11. Note that for each value of the electric permittivity, there is a electric potential limit at which we can apply the electric load. For the demonstration purpose, for each value of the electric permittivity we apply a potential difference $\psi_{upper} - \psi_{lower}$ close to this limit.

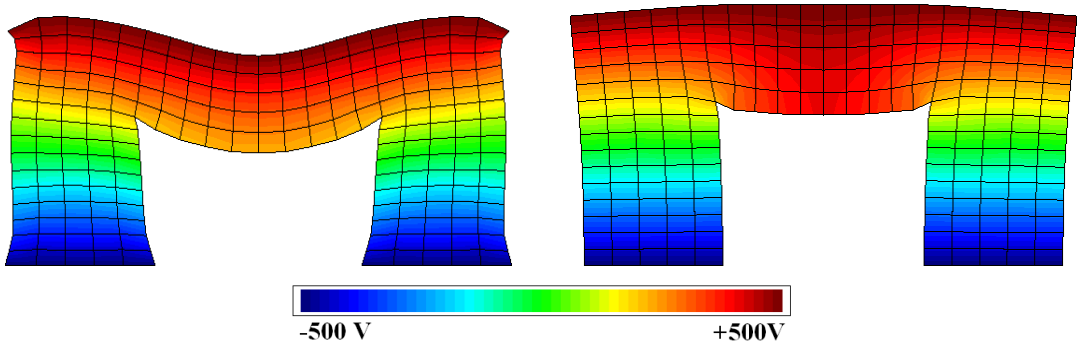

Fig. 8. Electric potential on deformed configuration using coupled BEM-FEM (left) and FEM (right): $\epsilon_m = 5.0\epsilon_0$.

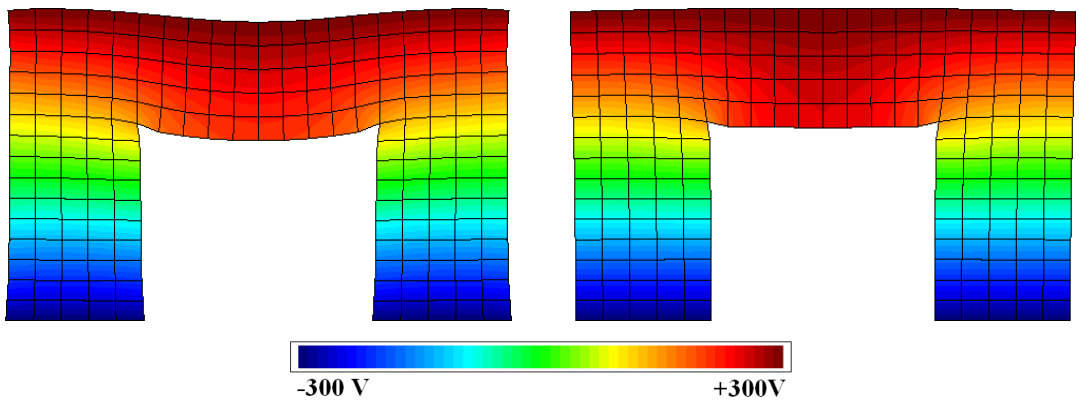

Fig. 9. Electric potential on deformed configuration using coupled BEM-FEM (left) and FEM (right): $\epsilon_m = 10.0\epsilon_0$.

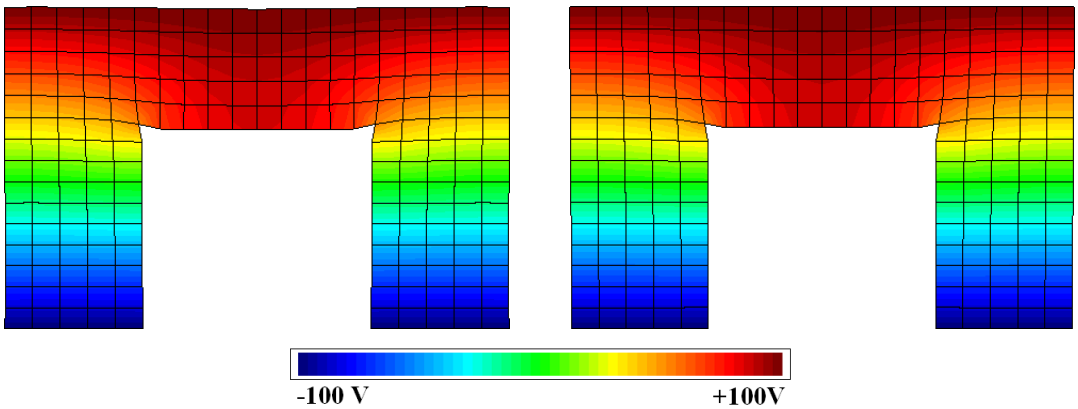

Fig. 10. Electric potential on deformed configuration using coupled BEM-FEM (left) and FEM (right): $\epsilon_m = 100.0\epsilon_0$.

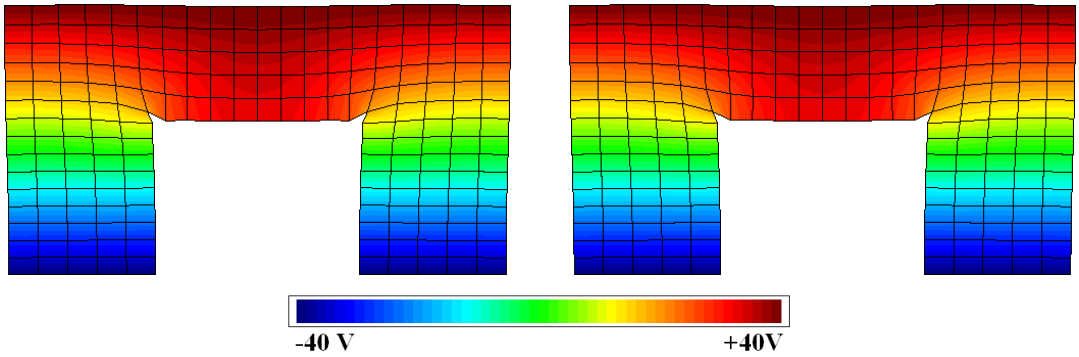

Fig. 11. Electric potential on deformed configuration using coupled BEM-FEM (left) and FEM (right): $\epsilon_m = 1000.0\epsilon_0$.

The numerical results lead us to a similar conclusion as in the case of zero deformation above: the smaller the electric permittivity the larger the difference between the results obtained by the two approaches. It can be observed that both electric tractions and electric fluxes play a significant role and the ignorance of these quantities might lead to very different simulation results.

For the second loading case, where an electric potential difference is placed between the internal and external edges of the plate, it is observed from the simulation results (Fig. 12) that the simulated electric potential obtained by using the coupled BEM-FEM approach and the one obtained by using the FEM approach are very similar. However, the simulated deformations (Fig. 13) give us a completely different picture. In this case it can be seen that the role of the electric traction is more important and is the main reason for the difference between the two simulation results.

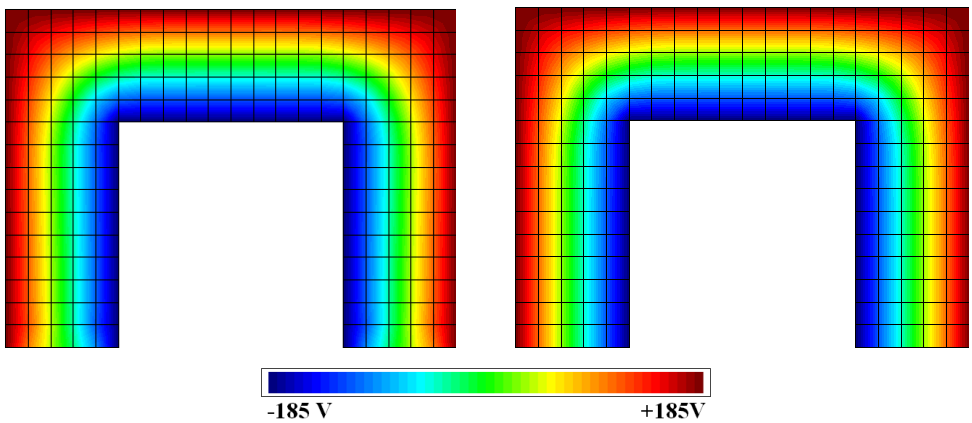

Fig. 12. Electric potential on undeformed configuration using coupled BEM-FEM (left) and FEM (right): $\epsilon_m = 5.0\epsilon_0$.

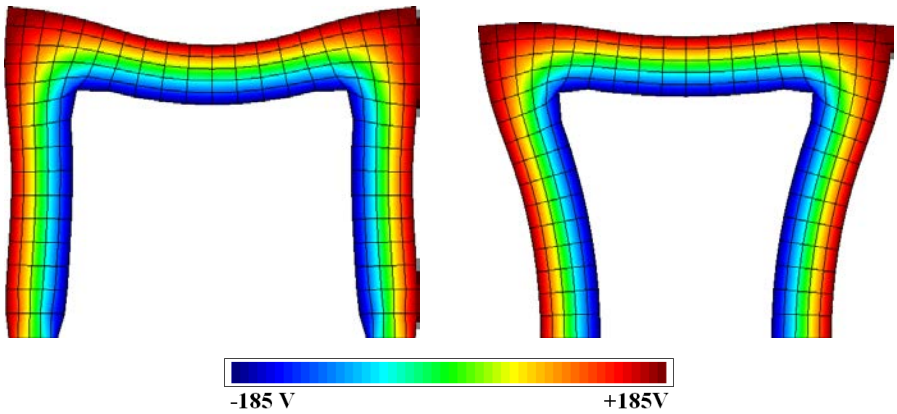

Fig. 13. Electric potential on deformed configuration using coupled BEM-FEM (left) and FEM (right): $\epsilon_m = 5.0\epsilon_0$.

5. Conclusion

The numerical modeling of nonlinear electroelasticity is clearly still a challenge today not only because of the complexity of the nonlinear coupled electro-mechanical characteristics but also because of the dimension of the problem. Evidently it should be noted that the influence of the free space on the electric field and the deformation field inside a material body depends on the one hand the material properties of the body and on the other hand the geometry of the body as well as the way an electric field is applied on to the body. However, in order to build a complete picture of what happens inside a nonlinear electroelastic body, what happens outside deserves a due attention.

Acknowledgments

The authors greatly acknowledge the financial support of the German Research Foundation (DFG) under the project "Electronic electroactive polymers under electric loading: Experiment, Modelling and Simulation", Grant Number: STE 544/36-1.

References

[1] C. Brebbia. *The boundary element method for engineers*. John Wiley & Sons, New York, 1978.
[2] J. Bonet and R.D. Wood. *Nonlinear continuum mechanics for finite element analysis*. Cambridge University Press, 1997.
[3] Q. Chen and A. Konrad. A review of finite element open boundary techniques for static and quasistatic electromagnetic field problems. *IEEE Transactions on Magnetics*, **33**: 663–676, 1997.
[4] A. Dorfmann and R.W. Ogden. Nonlinear electroelasticity. *Acta Mechanica*, **174**: 167–183, 2005.
[5] A.C. Eringen and G.A. Maugin. *Electrodynamics of continua. Volume 1 – Foundations and solid media*. Springer-Verlag, New York, 1989.
[6] R.M. McMeeking and C.M. Landis. Electrostatic forces and stored energy for deformable dielectric materials. *Journal of Applied Mechanics – American Society of Mechanical Engineers – ASME*, **72**: 581–590, 2005.
[7] P. Steinmann. Computational nonlinear electro-elasticity – Getting started. Lecture notes. *Mechanics and electrodynamics of magneto- and electro-elastic materials. CISM Summer School, International Centre for Mechanical Sciences*. Udine, Italy, June 29 – July 3, 2009.
[8] D.K. Vu and P. Steinmann. A 2-D coupled BEM-FEM simulation of electro-elastostatics at large strain. *Comput. Methods Appl. Mech. Engng.*, **199**: 1124–1133, 2010.
[9] D.K. Vu and P. Steinmann. On 3-D coupled BEM-FEM simulation of nonlinear electro-elastostatics. *Comput. Methods Appl. Mech. Engng.*, submitted for publication.
[10] D.K. Vu and P. Steinmann. Numerical simulation of electric electro-active polymers. *Proceedings, Sensor+Test Conferences 2011*, AMA Service GmbH, Germany, pp. 323–327, 2011
[11] D.K. Vu, P. Steinmann, G. Possart. Numerical modeling of nonlinear electroelasticity. *Int. J. Numer. Meth. Eng.*, **70**: 685–704, 2007.
[12] L.C. Wrobel. *The boundary element method. Volume 1: application in thermo-fluids and acoustics*. John Wiley & Sons, New York, 2002.